JointNull: Combining Reconfigurable Analog Cancellation with Transmit Beamforming for Large-antenna Full-duplex Wireless

Niranjan M Gowda and Ashutosh Sabharwal
Department of Electrical and Computer Engineering
Rice University, Houston, TX

Abstract

In this paper, we study the performance of a full-duplex architecture for large-antenna systems, where each receive antenna uses digital canceler but analog cancelers can be fewer in number than receive antennas. Analog cancelers are reconfigurable in the sense that they can be assigned to any antenna and convert it into a full-duplex antenna. We propose JointNull that jointly optimizes reconfigurable analog cancellation and transmit beamforming. JointNull assigns each antenna one of the three roles—full-duplex, half-duplex receive and half-duplex transmit antenna—and then designs a transmit precoder to suppress self-interference on receive antennas. We evaluate JointNull using channel measurements from an array with 72 antennas. We find that when combined with transmit beamforming, there is an optimal number of analog cancelers, less than total number of antennas, which achieve the maximum sum-rate. Further, JointNull achieves close to ideal full-duplex sum-rates using much fewer analog cancelers than the total number of antennas. For example, JointNull achieves 90% of ideal full-duplex sum-rate using only eight poor quality analog cancelers, each of which can cancel 20 dB of self-interference. Finally, rate region shows that when demand is highly biased towards downlink, JointNull achieves 90% of ideal sum-rate with even fewer or no analog cancelers.

Index Terms

Full-duplex system, massive MIMO, self-interference, transmit beamforming, analog cancelation.

An earlier version of this algorithm was also labeled JointNull, presented in [1], but considered only for the special case of zero analog cancellers. The journal version is significantly extended, with a new algorithm and new results.

The authors were partially supported by NSF grants CNS-1314822 and CNS-1518916.

I. INTRODUCTION

In-band full-duplex wireless, where a node can simultaneously send and receive in the same band, has the potential to nearly double the spectral efficiency of wireless networks [2]. A well-recognized challenge in enabling full-duplex is self-interference, where the transmissions of the node cause strong interference to its reception, potentially consuming the analog-to-digital converter's dynamic range and pushing the signal of interest below the quantization noise floor. To counter this challenge, there is now a rich and ever-growing literature on reducing self-interference in the analog domain, with techniques [3]–[11] that are collectively labeled as *analog cancelers*. The purpose of the analog cancelers is to reduce self-interference before the sum signal, self-interference and received signal of interest, reaches the analog-to-digital converter.

As the next generation cellular systems move to deploy a large number of antennas at the base-stations (e.g., 64-256 antenna configurations are being discussed in 3GPP [12]), analog cancelation based full-duplex poses a significant challenge due to a large associated analog complexity. To address the challenge of complexity of analog cancelation for large arrays, an alternative method called SoftNull [13] was proposed that relies only on transmit beamforming to reduce self-interference and in the process, *completely* eliminates the need for analog cancelers. SoftNull reconfigures the array elements into a transmit and a receive group (which can be done on a per-packet basis), sacrifices some transmit degrees-of-freedom to reduce self-interference, and in the process, enables full-duplex mode using current radio transceivers, i.e., achieve in-band full-duplex capability using only half-duplex TDD radios. While SoftNull completely eliminates analog cancelation and its associated complexity, full-duplex rate gains over half-duplex are no longer available in all cases. For example, in low-SNR outdoor cases, and high-scattering indoor environments, SoftNull rate gains over TDD are either very low or unavailable [13].

In this paper, we propose and study a self-interference cancelation architecture that spans the continuum between no analog cancelation (e.g. SoftNull) and full analog cancelation. Given the basic building block of an analog canceler that cancels the sum of self-interference impinging on an antenna in the analog domain, we propose the following architecture. For an array with M antennas, we propose an architecture with $N_{ac} \in [0, M]$ analog cancelers that can be used to make N_{ac} antennas full-duplex, while remaining $M - N_{ac}$ antennas are configured into transmit-only and receive-only groups; each such assignment of antenna roles is labeled as an *antenna*

configuration. The transmit group performs transmit beamforming to jointly optimize downlink data and self-interference reduction. The main question is two-fold: (i) *how* best should one utilize limited analog cancelation capabilities, and (ii) *what*, if any, are the rate gains from partial analog cancelation compared to the system based only on transmit beamforming. In this paper, we answer both questions via a new design called *JointNull*.

To answer the first question of *"how"*, we propose the JointNull algorithm to jointly design antenna configuration and transmit precoder. Since the overall design problem is of exponential complexity, JointNull divides the overall optimization into two phases to achieve polynomial complexity. The first phase designs the antenna configuration and the second phase designs a near-optimal precoder for the chosen configuration.

To answer the second question of *"what gains"*, we study the rate gains as a function of analog complexity, i.e., as N_{ac} increases from 0 to M. We investigate how the quality and number of analog cancelers impact overall performance. We model the *quality* of an analog canceler by the amount of average self-interference cancelation; higher numbers mean a better analog canceler. Our evaluation uses the open-access propagation dataset [1] collected by the authors of [13] from a 72-element array. The dataset is collected in multiple environments, including an anechoic chamber, high-scattering indoor and low-scattering outdoor environments. The key observations from our data-driven analysis are as follows.

Consider the case when $N_{ac} = 0$, the case considered by SoftNull [13]. We show that JointNull outperforms SoftNull for all antenna configurations, with gains as high as 15 dB. The gains can be attributed to the fact that the JointNull precoders jointly optimize self-interference suppression and downlink beamforming; in contrast, SoftNull decouples self-interference suppression from downlink precoding. Next, consider the case of $N_{ac} > 0$ cancelers. Intuitively one will conclude that overall sum-rate should increase monotonically with the number of analog cancelers. However, we discover that the rate gain is not monotonic and in fact, depending on *quality* of cancelers, the maximal rate achieved with analog cancelation combined with transmit precoding can be with N_{ac} strictly less than the total number of antennas M. The maxima-achieving number N_{ac}^* for JointNull depends on analog canceler quality. For example, when analog cancelers cancel only 20 dB of self-interference per antenna, the sum rate reaches its maximum when $N_{ac} \sim M/2$ and thereafter decreases with the increase in N_{ac}. However, for better cancelers, which can cancel

[1] http://fullduplex.rice.edu/datasets

60 dB, the maxima is achieved with $N_{ac} \sim M$ for the measured data with $M = 72$.

We then use the rate results to answer how many cancelers suffice to achieve a sum-rate that is close to the ideal full-duplex. We find that even with 20 dB analog cancelers, $N_{ac} \approx \frac{M}{10}$ suffice to be within 10% of maximum sum-rate. That means, eight 20 dB cancelers for a 72 antenna array can achieve 90% of ideal full-duplex when combined with transmit precoding. If the traffic demand is highly skewed towards downlink, for example when downlink demand is five times the uplink demand, the achievable downlink rate with $N_{ac} = 0$ is within 1% of the maximum achievable downlink rate; that is, no analog cancelers are needed in some cases of traffic demand.

The rest of the paper is organized as follows. In Section II, we provide the system model and formulate the problem. In Section III, we design JointNull and analytically investigate a few of its components. In Section IV, experimental evaluation results are discussed and JointNull is compared with previously known half/full-duplex schemes. Section V provides the conclusion.

Notations: We use bold uppercase and lowercase letters for denoting matrices and column vectors, respectively; † (as superscript) for Moore-Penrose pseudo inverse; $\|\cdot\|_F$ for Frobenius norm; $\|\cdot\|_2$ for l_2-norm; $|\cdot|$ for absolute value of a number and also for the cardinality of a set; $\circ$ for Hadamard product; $\mathcal{S}_1 \setminus \mathcal{S}_2$ for set minus; $\mathbf{I}_n$ for $n \times n$ identity matrix and $\mathbf{H}(\mathcal{S}_r, \mathcal{S}_c)$ represents the submatrix of matrix $\mathbf{H}$ constructed from the rows and columns indexed by the sets $\mathcal{S}_r$ and $\mathcal{S}_c$, respectively.

II. System model and problem statement

A. Flexible Antenna Configuration

We consider a base station with a rectangular antenna array of M_{row} rows, M_{col} columns and $M = M_{row}M_{col}$ antennas. Each antenna can operate in one of the three modes: full-duplex, transmit-only and receive-only. In the sequel, we will refer to transmit-only antennas as half-duplex transmit, receive-only as half-duplex receive antennas, and rest as full-duplex antennas. As described below, the flexibility lies in assigning any antenna to one of the above three modes of operation, thereby changing the configuration of the whole array.

We will assume that the base-station has N_{ac} analog cancelers, each of which can be used with any of the M antennas to convert it into a full-duplex antenna capable of simultaneous transmission and reception in the same frequency band. We will denote the number of transmit and receive antennas as M_t and M_r, respectively; see example configurations in the Figure 1.

With the above setup, the number of half-duplex transmit and receive antennas are, $M_t - N_{ac}$ and $M_r - N_{ac}$, respectively. And thus the parameters are related as $M = M_t + M_r - N_{ac}$. We assume that an analog canceler can cancel β_{ac} dB of self-interference on each antenna. As we will consider analog-cancelers that will partially cancel the self-interference, $\beta_{ac} < \infty$; note that none of the reported analog cancelers cancel self-interference completely.

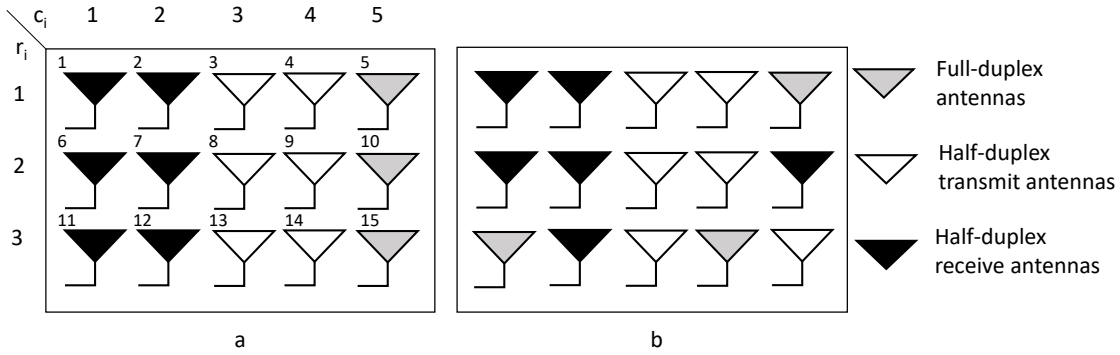

Fig. 1: *Two example configurations for an array with* $M = 15$*, with* $N_{ac} = 3$ *analog cancelers. For each configuration,* $M_r = M_t = 9$*.*

For the ease of exposition, we assume that the network has the same number of downlink and uplink users. Let the total number of users be $2K$ with K uplink and K downlink users, such that $K < \min\{M_t, M_r\}$. We assume that there is no interference on the downlink users from the uplink users and that all the channels are block fading. Let $\mathbf{H}_D \in \mathbb{C}^{K\times M}$, $\mathbf{H}_U \in \mathbb{C}^{M\times K}$ and $\mathbf{H}_S \in \mathbb{C}^{M\times M}$ be the downlink, uplink and self-interference channels, respectively. The matrix $\mathbf{H}_S$ represents uncanceled self-interference between any two antennas before they are assigned any roles.

We introduce the following variables to formally state the signal model and problem formulation.

1) An antenna is represented by an ordered pair, (r_i, c_i), where $0 \le r_i \le M_{row}$, $0 \le c_i \le M_{col}$. The ordered pair, (r_i, c_i), gives the location of the antenna in the rectangular array. For example, the full-duplex antennas in Figure 1b are represented by $(1, 5), (3, 1)$ and $(3, 4)$.
2) We also represent an antenna by a unique integer from the set $\{1, 2, \cdots, M\}$. The function, $f : \{(r_i, c_i) : 0 \le r_i \le M_{row} \text{ and } 0 \le c_i \le M_{col}\} \to \{1, 2, \cdots, M\}$, gives the one-to-one mapping between the two representation of an antenna element. For example, the full

duplex antennas in Figure 1b are represented by $\{5, 11, 14\}$ and $f(\{(1,5),(3,1),(3,4)\}) = \{5, 11, 14\}$.

3) The index sets of full-duplex, half-duplex transmit and half-duplex receive antennas are denoted by, $\mathcal{S}_{FD}$, $\mathcal{S}_{HDT}$ and $\mathcal{S}_{HDR} \subset \{(r_i, c_i) : 0 \leq r_i \leq M_{row} \text{ and } 0 \leq c_i \leq M_{col}\}$, respectively, for a given configuration. The sets are disjoint and their cardinalities are, respectively, N_{ac}, $M_t - N_{ac}$ and $M_r - N_{ac}$. The union of the sets, $\mathcal{S}_{FD} \bigcup \mathcal{S}_{HDT} \bigcup \mathcal{S}_{HDR} = \{(r_i, c_i) : 0 \leq r_i \leq M_{row} \text{ and } 0 \leq c_i \leq M_{col}\}$. Hence, any two of the sets are sufficient to uniquely specify a configuration. We choose the index sets for half-duplex transmit and full-duplex antennas, $(\mathcal{S}_{HDT}, \mathcal{S}_{FD})$, to represent a configuration.

4) For a given configuration specified by $(\mathcal{S}_{HDT}, \mathcal{S}_{FD})$, the uplink, downlink and self-interference channels are, respectively, given by,

$$\begin{aligned}
\mathbf{H}_u &= \mathbf{H}_U(f\{\mathcal{S}_{HDR} \bigcup \mathcal{S}_{FD}\}, :) \in \mathcal{C}^{M_r \times K}, \\
\mathbf{H}_d &= \mathbf{H}_D(:,\ f\{\mathcal{S}_{HDT} \bigcup \mathcal{S}_{FD}\}) \in \mathcal{C}^{K \times M_t}, \text{ and} \\
\mathbf{H}_s &= \mathbf{T} \circ \mathbf{H}_S(f\{\mathcal{S}_{HDR} \bigcup \mathcal{S}_{FD}\},\ f\{\mathcal{S}_{HDT} \bigcup \mathcal{S}_{FD}\}) \in \mathcal{C}^{M_r \times M_t},
\end{aligned} \tag{1}$$

where $\mathbf{T}$ is such that,

$$\mathbf{T}_{ij} = \begin{cases} 10^{-\beta_{ac}/20} & \text{if } f^{-1}(i) \in \mathcal{S}_{FD} \text{ or } f^{-1}(j) \in \mathcal{S}_{FD} \\ 0 & \text{if } i = j \text{ and } f^{-1}(i) \notin \mathcal{S}_{FD} \\ 1 & \text{otherwise} \end{cases}. \tag{2}$$

Matrix $\mathbf{T}$ scales down the self-interference on full-duplex antennas by β_{ac} dB, amount equal to the analog cancelation.

In the sequel, we slightly abuse the notation and drop $f\{\cdot\}$ in the future. It is implicitly assumed that f or f^{-1} are involved whenever an ordered pair is used to specify an antenna instead of an integer or vice versa.

5) Since the set of all configurations is countable, we differentiate the configurations by using indexed tuples, $(\mathcal{S}^n_{HDT}, \mathcal{S}^n_{FD})$. We use indexed tuples in the discussions, whenever there is a need to differentiate between multiple configurations. Let $\mathbb{B}$ be the set that contains the tuples of all $\binom{M}{N_{ac}}2^{M-N_{ac}}$ configurations. i.e., $\mathbb{B} = \{(\mathcal{S}^n_{HDT}, \mathcal{S}^n_{FD}) : n = 1, \cdots, \binom{M}{N_{ac}}2^{M-N_{ac}}\}$.

B. Signal Model

We assume that the transmit signal at the base station is always precoded with a precoder, $\mathbf{P}$. For the configuration given by $(\mathcal{S}_{HDT}, \mathcal{S}_{FD})$, the signals received at mobile users and base-station are, respectively, given by

$$\mathbf{y}_d = \mathbf{H}_d \mathbf{P} \mathbf{x}_d + \mathbf{w}_d, \tag{3}$$

$$\mathbf{y}_u = \mathbf{H}_u \mathbf{x}_u + \mathbf{H}_s \mathbf{P} \mathbf{x}_d + \mathbf{w}_u, \tag{4}$$

where, $\mathbf{x}_d \in \mathbb{C}^{K\times 1}$ is the transmit signal at the base station before precoding, $\mathbf{x}_u \in \mathbb{C}^{K\times 1}$ is the signal from all the uplink users, $\mathbf{y}_d \in \mathbb{C}^{K\times 1}$ is the signal received by all the K downlink users and $\mathbf{y}_u \in \mathbb{C}^{M_r\times 1}$ is the signal received at the base station; the noise vectors $\mathbf{w}_d \sim \mathcal{CN}(0, \sigma_d^2 \mathbf{I}_K)$ and $\mathbf{w}_u \sim \mathcal{CN}(0, \sigma_u^2 \mathbf{I}_{M_r})$. We assume that the transmit power of the base-station and users do not exceed unity i.e., $E[\|\mathbf{P}\mathbf{x}_d\|_2^2] \leq 1$ and $E[\|\mathbf{x}_u\|_2^2] \leq 1$. We let $E[\|\mathbf{x}_d\|_2^2] = K$ and hence $\|\mathbf{P}\|_F^2 \leq 1$. We consider only full-rank channel matrices, inspired by the recent measurement results [14].

C. Problem Statement

In this paper, we study the solution for full-duplex designs that use a combination of (i) transmission precoding, (ii) partial analog cancelation with $N_{ac} \leq M$ analog cancelers, and (iii) digital cancelation for managing self-interference. In this paper, we adopt a demand-based objective,[2] where the antenna configuration and precoder are designed to meet the uplink-downlink user demand rate tuple $(\alpha_u^{dem}, \alpha_d^{dem})$ bits/s/Hz. We aim to find the antenna configuration and the transmit zero-forcing precoder that minimizes the gap between the demand and achievable rates. Let α_u and α_d be an achievable uplink and downlink rate pair. The optimization problem for finding the configuration and transmit precoder with an objective of meeting the demand rates as closely as possible is given as

$$\begin{aligned} \min \ & |\alpha_u^{dem} - \alpha_u| + |\alpha_d^{dem} - \alpha_d| \\ \text{such that } & \mathbf{H}_d \mathbf{P} = c\mathbf{I}, \\ & \|\mathbf{P}\|_F^2 \leq 1, \\ & (\mathcal{S}_{HDT}, \mathcal{S}_{FD}) \in \mathbb{B},\ 0 \leq M_t \leq M,\ c \in \mathbb{R}^+, \end{aligned} \tag{5}$$

[2]This is only one of the possible objective functions for the configuration and precoder design; different objectives will lead to different designs.

where,

$$\alpha_u = K \log_2 \left(1 + \underbrace{\frac{\|\mathbf{H}_u\|_F^2}{K(\sigma_u^2 + 10^{-\beta_{dc}/10}\|\mathbf{H}_s\mathbf{P}\|_F^2)}}_{\text{uplink SINR}} \right),$$

$$\alpha_d = K \log_2 \left(1 + \underbrace{\frac{\|\mathbf{H}_d\mathbf{P}\|_F^2}{K\sigma_d^2}}_{\text{downlink SNR}} \right), \tag{6}$$

where relations between $\mathbf{H}_d$, $\mathbf{H}_u$, $\mathbf{H}_s$, M_t and $(\mathcal{S}_{HDT}, \mathcal{S}_{FD})$ are given in (1) and β_{dc} is the amount of digital self-interference cancelation.

The constraints in optimization problem (5) are for a zero-forcing transmit precoder and satisfies max-min fairness criterion for the downlink users. Furthermore, the precoder satisfies max-min fairness criterion to ensure that all downlink users receive their respective signals from the base-station with equal power. The matrix, $\mathbf{H}_d\mathbf{P}$, is a diagonal matrix with non-negative diagonal entries as $\mathbf{P}$ is zero-forcing. Further, since $\mathbf{P}$ satisfies max-min fairness criterion, all the diagonal entries of $\mathbf{H}_d\mathbf{P}$ are equal i.e., $\mathbf{H}_d\mathbf{P} = c\mathbf{I}$, where $c \geq 0$, which is the first constraint in (5). For any other criteria, like max-throughput, the diagonal entries could be unequal.

The self-interference power before and after digital cancelation are, $\|\mathbf{H}_s\mathbf{P}\|_F^2$ and $10^{-\beta_{dc}/10}\|\mathbf{H}_s\mathbf{P}\|_F^2$, respectively. We have used an objective function that minimizes the ℓ_1-distance between the achievable and demand rates. However, any other distance metric, such as ℓ_2-norm, can be used in the objective. The proposed solution in section III would require no other changes except for changing the distance metric to the one used in the objective.

III. JointNull for Massive MIMO full-duplex

For an array with M antennas and N_{ac} analog cancelers, there are $\binom{M}{N_{ac}} \times 2^{M-N_{ac}}$ unique configurations. In each configuration, there would be $M - N_{ac}$ half-duplex antennas which are configured into $M_t - N_{ac}$ half-duplex transmit and $(M - M_t + N_{ac})$ half-duplex receive antennas, where $M_t \in \{N_{ac}, N_{ac}+1, \cdots, M\}$. Hence, finding the optimal configuration has exponential complexity. Thus, we propose a sub-optimal polynomial complexity antenna configuration algorithm for the problem in (5). The proposed algorithm, *JointNull*, divides the optimization into two main steps: *configuration design* and *precoder design*. The configuration design is the suboptimal step due to the combinatorial nature of the problem. Once the array is configured, we design near-optimal precoders for that configuration.

We first give an overview of JointNull algorithm and its components in section III-A. Section III-B describes the configuration design algorithm and section III-C describes precoder design algorithm.

A. Overview of JointNull

The objective function in (5) can be rewritten as,

$$f(\mathcal{S}_{HDT}, \mathcal{S}_{FD}, \mathbf{P}) = \left| \alpha_u^{dem} - K \log_2 \left(1 + \frac{\|\mathbf{H}_u\|_F^2}{K(\sigma_u^2 + \beta_{si}\|\mathbf{H}_s\mathbf{P}\|_F^2)} \right) \right| + \left| \alpha_d^{dem} - K \log_2 \left(1 + \frac{\|\mathbf{H}_d\mathbf{P}\|_F^2}{K\sigma_d^2} \right) \right| \quad (7)$$

where the sets $\mathcal{S}_{HDT}$ and $\mathcal{S}_{FD}$ contain the indices of the half-duplex transmit and full-duplex antennas, respectively. The uplink, downlink and self-interference channel matrices are determined by the configuration given by the tuple $(\mathcal{S}_{HDT}, \mathcal{S}_{FD})$ as follows. The half-duplex receive antennas are, $\mathcal{S}_{HDR} = \{(r_i, c_i) : 0 \leq r_i \leq M_{row} \text{ and } 0 \leq c_i \leq M_{col}\} \setminus (\mathcal{S}_{HDT} \cup \mathcal{S}_{FD})$. The uplink, downlink and self-interference channel matrices are then given by (1). Since noise variance and number of users are fixed in our system, the uplink rate is a function of the self-interference power, $P_{si} = \|\mathbf{H}_s\mathbf{P}\|_F^2$ and the sum of the power of all uplink users' signal received by the base station, $P_{ul} = \|\mathbf{H}_u\|_F^2$. The downlink rate is a function of sum of all users' downlink receive power, $P_{dl} = \|\mathbf{H}_d\mathbf{P}\|_F^2$.

The self-interference power, downlink receive power and uplink receive power, $P_{si},\ P_{dl}$ and P_{ul}, respectively, are all inter-related as follows. For a fixed $\mathbf{H}_U$, the uplink receive power, P_{ul}, depends solely on the configuration specified by $(\mathcal{S}_{HDT}, \mathcal{S}_{FD})$. The downlink receive power and self-interference power depend on both the configuration, $(\mathcal{S}_{HDT}, \mathcal{S}_{FD})$, and the precoder, $\mathbf{P}$, for a fixed $\mathbf{H}_S$ and $\mathbf{H}_D$. To reduce complexity, rather than trading off all the three powers jointly, JointNull first optimizes tradeoff between P_{dl} and P_{ul} in configuration design step, and then optimizes the trade-off between P_{dl} and P_{si} in the precoder design step.

The configuration design algorithm considers only those configurations that facilitate the precoder design step to better suppress self-interference. The chosen configuration determines the uplink receive power and the maximum downlink receive power and is based on the data-driven observations in [13].

In the precoder design step, optimal precoders are designed for a small, finite set of downlink receive powers that range between zero and the maximum downlink receive power for the chosen

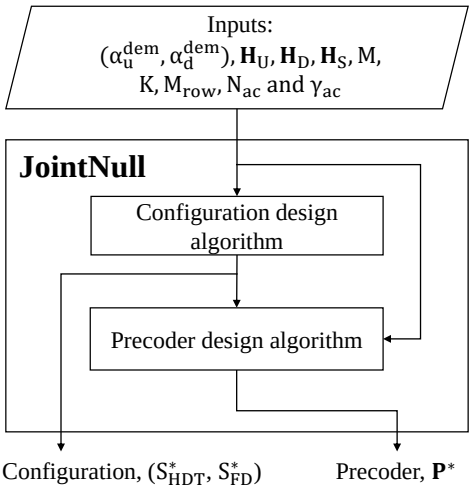

Fig. 2: *An outline of the JointNull algorithm*

configuration. Then a precoder is chosen whose self-interference and downlink receive power are closest to the desired values. Figure 2 outlines the JointNull algorithm.

B. JointNull configuration design algorithm

In this section, we propose a polynomial time algorithm to choose a configuration from the set of $\binom{M}{N_{ac}} \times 2^{M-N_{ac}}$ configurations. We first choose a subset of configurations which facilitate the suppression of a large amount of self-interference in the precoder design step. We denote by set, $\mathcal{B}_{JN}$, the reduced set of configurations. Then, we choose one configuration from $\mathcal{B}_{JN}$ based on demand rate and channel conditions.

The construction of $\mathcal{B}_{JN}$ is given by Algorithm 3 in appendix B. The cardinality of $\mathcal{B}_{JN}$ is polynomial in M. In each configuration of $\mathcal{B}_{JN}$, there are M_t transmit and $M - M_t + N_{ac}$ receive antennas. The reduction in cardinality is achieved by considering only the configurations which have the fewest number of half-duplex receive antennas that neighbor the transmit antennas and have contiguous half-duplex transmit antennas. The half-duplex transmit antennas that maximize receive diversity are then chosen as full-duplex antennas. Minimizing the number of half duplex receive antennas adjacent to transmit antennas, minimizes the receive antennas which are severely affected by self-interference. Further, self-interference on the rest of the half-duplex receive antennas, which are farther away from the group of transmit antennas, would be less severe as pathloss would be higher. The contiguousness of transmit antennas helps precoders to efficiently

suppress self-interference by allowing all transmit antennas to create low power beams at receive antennas in a few common directions. Typically, to achieve similar levels of self-interference, a configuration with non-contiguous transmit antennas would have to create low power beams in more directions than that of a configuration with contiguous transmit antennas [13]. In short, the configurations in $\mathcal{B}_{JN}$ potentially allow precoders to suppress a large amount of self-interference on half-duplex receive antennas and exploit full-duplex antennas to achieve better receive diversity.

The maximum uplink and downlink rates for a configuration depend on the downlink, uplink and self-interference channels experienced by the transmit and receive antennas of the configuration. The configuration design algorithm should choose a configuration such that its maximum uplink and downlink rates are as large as possible, relative to the uplink and downlink demand rates, (α_u^{dem} and α_d^{dem}). For example, when the downlink demand is higher than uplink demand, a configuration which has a larger number of transmit antennas than the number of receive antennas is more likely to satisfy the demand than the one with a lesser number of transmit antennas. When there are several configurations whose maximum rates are greater than demand, it is preferable to choose the one which has the largest number of transmit antennas and whose maximum rates are the farthest from the demand rates, as the achievable rates are bound to go less than the maximum rates while managing the self-interference. If there exists no configuration whose maximum rates are greater than demand, then we seek the partition whose maximum rates are closest to the demand.

The parameters that remain constant for a fixed configuration are uplink receive power, P_{ul}, and the channel matrices, $\mathbf{H}_d, \mathbf{H}_u$ and $\mathbf{H}_s$. For a fixed P_{ul}, the maximum achievable uplink rate is obtained by assuming zero-self-interference in the uplink SINR expression in (6). For a fixed downlink channel matrix, $\mathbf{H}_d$, the Moore-Penrose precoder, $\mathbf{P}^{\dagger} = \mathbf{H}_d^H(\mathbf{H}_d\mathbf{H}_d^H)^{-1}/\|\mathbf{H}_d^H(\mathbf{H}_d\mathbf{H}_d^H)^{-1}\|_F$, results in the maximum downlink receive power among all zero-forcing unit-norm precoders [15]. Hence, the maximum downlink rate, $\alpha_{d,max}^n$, is obtained by using Moore-Penrose precoder, $\mathbf{P}^{\dagger}$, with downlink SNR expression given by (6). The antenna configuration design algorithm is given in Algorithm 1.

Step 3 of configuration design algorithm corresponds to the case where demand is less than the maximum achievable rates. In this case, the configuration with the largest downlink receive power is chosen. For the precoders used by JointNull, self-interference power decreases monotonically with decreasing downlink receive power (see Subsection III-C). Hence, the precoders

Algorithm 1 Configuration design algorithm

Initialization: Let each configuration in $\mathcal{B}_{JN}$ be assigned with a unique number from the set $\{1, \cdots, |\mathcal{B}_{JN}|\}$. Then, $\mathcal{B}_{JN} = \{(\mathcal{S}^n_{HDT}, \mathcal{S}^n_{FD}) : n = 1, \cdots, |\mathcal{B}_{JN}|\}$.

Output: Configuration, $(\mathcal{S}^*_{HDT}, \mathcal{S}^*_{FD}) \in \mathcal{B}_{JN}$

1: Compute maximum achievable rates of the configurations in $\mathcal{B}_{JN}$. Let them be, $(\alpha^n_{u,max}, \alpha^n_{d,max})$, where $n = 1, \cdots, |\mathcal{B}_{JN}|$. Let M^n_t be the number of transmit antennas in n^{th} configuration.

2: Construct $\mathcal{I} \subset \{1, \cdots, |\mathcal{B}_{JN}|\}$, such that $\alpha^{dem}_u \leq \alpha^n_{u,max}$ and $\alpha^{dem}_d \leq \alpha^n_{d,max}$ for all $n \in \mathcal{I}$.

3: **if** $\mathcal{I} \neq \Phi$ **then**

$$\mathcal{I}' = \{m : m = \arg\max_{n \in \mathcal{I}} \ M^n_t\} \text{ and } \ n^* = \arg\max_{n \in \mathcal{I}'} \ \alpha^n_{d,max}$$

4: **else** $n^* = \arg\min_{n=1,\cdots,|\mathcal{B}_{JN}|} |\alpha^{dem}_u - \alpha^n_{u,max}| + |\alpha^{dem}_d - \alpha^n_{d,max}|$

5: **end if**

6: $(\mathcal{S}^*_{HDT}, \mathcal{S}^*_{FD}) \leftarrow (\mathcal{S}^{n^*}_{HDT}, \mathcal{S}^{n^*}_{FD})$

can suppress a larger amount of self-interference for the configuration with the largest downlink receive power than that for other configurations.

Step 4 of configuration design algorithm addresses the case when the demand is beyond the maximum achievable rates. In such a case, JointNull chooses the configuration whose maximum achievable rates are closest to the demand, in l_1-distance sense.

C. JointNull Precoder design algorithm

Precoder design step controls the achievable uplink and downlink rates through the precoder, **P**, as the rest of the parameters are fixed once the configuration is chosen. The precoder design step has to balance between self-interference power (P_{si}) and downlink receive power (P_{dl}), such that the resulting rates are close to or greater than demand rates. To achieve the above goal, we first state a convex problem to design self-interference suppressing precoders. The self-interference suppressing precoder is an optimal precoder that minimizes self-interference for a fixed downlink receive power. We then give an algorithm to design a precoder that near-optimally trades off P_{si} and P_{dl} using self-interference suppressing precoders.

1) Precoder design with fixed downlink receive power as a convex optimization problem: We express $\mathbf{H}_S$ as the sum of a diagonal matrix, $\mathbf{D}_S$, and a matrix whose diagonal entries are all zeros, $\overline{\mathbf{H}}_S$,

$$\mathbf{H}_S = \overline{\mathbf{H}}_S + \mathbf{D}_S \tag{8}$$

$$\implies \mathbf{H}_s = \mathbf{T} \circ \mathbf{H}_S(\mathcal{S}_{HDR} \bigcup \mathcal{S}_{FD},\ \mathcal{S}_{HDT} \bigcup \mathcal{S}_{FD}) \tag{9}$$

$$= \mathbf{T} \circ \overline{\mathbf{H}}_S(\mathcal{S}_{HDR} \bigcup \mathcal{S}_{FD},\ \mathcal{S}_{HDT} \bigcup \mathcal{S}_{FD}) + \tag{10}$$

$$\mathbf{T} \circ \mathbf{D}_S(\mathcal{S}_{HDR} \bigcup \mathcal{S}_{FD},\ \mathcal{S}_{HDT} \bigcup \mathcal{S}_{FD}) \tag{11}$$

Let $\overline{\mathbf{H}}_s = \mathbf{T} \circ \overline{\mathbf{H}}_S(\mathcal{S}_{HDR} \bigcup \mathcal{S}_{FD},\ \mathcal{S}_{HDT} \bigcup \mathcal{S}_{FD})$ and $\mathbf{D}_s = \mathbf{T} \circ \mathbf{D}_S(\mathcal{S}_{HDR} \bigcup \mathcal{S}_{FD},\ \mathcal{S}_{HDT} \bigcup \mathcal{S}_{FD})$. Each row of the matrix $\overline{\mathbf{H}}_s$ denotes the self-interference on an antenna due to the transmissions from other antennas. The matrix, $\mathbf{D}_s$, has $|\mathcal{S}_{FD}|$ non-zero entries, and each non-zero entry denotes the self-interference at a full-duplex antenna due to its own transmissions. Beamforming, realized using precoders, can suppress $\overline{\mathbf{H}}_s$, but cannot suppress $\mathbf{D}_s$. Hence, precoders are designed to suppress only $\overline{\mathbf{H}}_s$.

Let $\mathbf{R} \in \mathbb{C}^{M_t \times K}$ be any right inverse of $\mathbf{H}_d$ and $\mathbf{H}_d^\dagger = \mathbf{H}_d^H(\mathbf{H}_d\mathbf{H}_d^H)^{-1}$ be the Moore-Penrose right inverse. $\mathbf{H}_d^\dagger$ is orthogonal to the null space of $\mathbf{H}_d$. Hence, a right-inverse can be written as the sum of $\mathbf{H}_d^\dagger$ and a matrix constructed from the vectors of null-space of $\mathbf{H}_d$,

$$\mathbf{R} = \mathbf{H}_d^\dagger - \mathbf{H}_n\mathbf{X}, \tag{12}$$

where $\mathbf{H}_n \in \mathbb{C}^{M_t \times M_t - K}$ is an orthonormal matrix whose columns span the null-space of $\mathbf{H}_d$ and $\mathbf{X} \in \mathbb{C}^{M_t - K \times K}$. Each distinct $\mathbf{X}$ will generate a unique right-inverse of $\mathbf{H}_d$. The max-min fairness for downlink users always results in equal downlink receive power for all the users i.e., $\mathbf{H}_d\mathbf{P}$ would be a diagonal matrix with equal diagonal entries. Hence, zero-forcing precoders that satisfy max-min fairness are always the right inverses of $\mathbf{H}_d$, scaled with a positive real number.

$$\mathbf{P} = \sqrt{p_{dl}}(\mathbf{H}_d^\dagger - \mathbf{H}_n\mathbf{X}),\ \text{where } \mathbf{X} \in \mathbb{C}^{M_t - K \times K} \text{ and } p_{dl} \geq 0 \tag{13}$$

where $p_{dl} = P_{dl}/K$, the receive power at each downlink user. The transmit power at the base-station after precoding would be $p_{dl}\|\mathbf{H}_d^\dagger - \mathbf{H}_n\mathbf{X}\|_F^2$. The self-interference power, with $\mathbf{P}$ as the precoder is,

$$P_{si} = \|\overline{\mathbf{H}}_s\mathbf{P}\|_F^2 = p_{dl}\|\overline{\mathbf{H}}_s\mathbf{H}_d^\dagger - \overline{\mathbf{H}}_s\mathbf{H}_n\mathbf{X}\|_F^2 \tag{14}$$

For a fixed per-user downlink receive power, p_{dl}, minimizing (14) with a constraint on transmit power results in a constrained least-squares problem and is given in (15).

$$\mathbf{X}^* = \begin{cases} \min\limits_{\mathbf{X}} & \|\overline{\mathbf{H}}_s(\mathbf{H}_d^\dagger - \mathbf{H}_n\mathbf{X})\|_F \\ \text{s.t.} & \sqrt{p_{dl}}\|\mathbf{H}_d^\dagger - \mathbf{H}_n\mathbf{X}\|_F \leq 1 \end{cases} \tag{15}$$

The precoder constructed from (15), $\mathbf{P}^* = \sqrt{p_{dl}}(\mathbf{H}_d^\dagger - \mathbf{H}\mathbf{X}^*)$, maximally suppresses the self-interference or equivalently, minimizes the self-interference power, for a fixed p_{dl}. We refer to the precoder $\mathbf{P}^*$ as *self-interference suppressing precoder*. The constraint in (15) ensures that the average transmit power does not exceed unity.

For any right inverse $\mathbf{R} \neq \mathbf{H}_d^\dagger$, $\|\mathbf{H}_d^\dagger\|_F < \|\mathbf{R}\|_F$ [15], where $\mathbf{H}_d^\dagger$ is the Moore-Penrose right inverse. Hence,

$$\frac{\|\mathbf{H}_d\mathbf{H}_d^\dagger\|_F}{\|\mathbf{H}_d^\dagger\|_F} = \frac{\sqrt{K}}{\|\mathbf{H}_d^\dagger\|_F} > \frac{\sqrt{K}}{\|\mathbf{R}\|_F} = \frac{\|\mathbf{H}_d\mathbf{R}\|_F}{\|\mathbf{R}\|_F} \tag{16}$$

$\forall\ \mathbf{R} \neq \mathbf{H}_d^\dagger$. Therefore, p_{dl} in (15) cannot exceed that of Moore-Penrose precoder, $\mathbf{P}^\dagger = \mathbf{H}_d^\dagger/\|\mathbf{H}_d^\dagger\|_F$ i.e., $\mathbf{P}^\dagger$ delivers the maximum power to users among all the zero-forcing precoders, under max-min fairness. Let the per-user downlink receive-power with $\mathbf{P}^\dagger$ as the precoder be $p_{dl}^\dagger$. Then, the per-user downlink receive power p_{dl} for (15) is upper bounded by $p_{dl}^\dagger$,

$$p_{dl} \leq p_{dl}^\dagger = \frac{1}{\|\mathbf{H}_d^\dagger\|_F^2}. \tag{17}$$

The problem in (15) would be infeasible when $p_{dl} > p_{dl}^\dagger$ since $\sqrt{p_{dl}}\|\mathbf{H}_d^\dagger - \mathbf{H}_n\mathbf{X}\|_F > 1$ for all $\mathbf{X} \in \mathbb{C}^{M_t - K \times K}$

Self-interference power monotonically decreases with decreasing downlink receive power, when solutions of (15) are used as the precoders. As proof, let $\widehat{p}_{dl} \leq \widetilde{p}_{dl}$ and the corresponding precoders obtained from (15) be $\widehat{\mathbf{P}}$ and $\widetilde{\mathbf{P}}$, respectively. Let $\widehat{P}_{si} = \|\overline{\mathbf{H}}_s\widehat{\mathbf{P}}\|_F^2$ and $\widetilde{P}_{si} = \|\overline{\mathbf{H}}_s\widetilde{\mathbf{P}}\|_F^2$, the self-interference powers due to $\widehat{\mathbf{P}}$ and $\widetilde{\mathbf{P}}$ respectively. $\widehat{P}_{si}$ cannot exceed $\widetilde{P}_{si}$, otherwise for the downlink receive power $\widehat{p}_{dl}$, the precoder $\widetilde{\mathbf{P}} \times \sqrt{\widehat{p}_{dl}/\widetilde{p}_{dl}}$ would result in lower self-interference than $\widehat{P}_{si}$. Therefore, $\widehat{P}_{si} \leq \dfrac{\widehat{p}_{dl}}{\widetilde{p}_{dl}}\widetilde{P}_{si}$.

Further, since $\widehat{P}_{si} \leq \dfrac{\widehat{p}_{dl}}{\widetilde{p}_{dl}}\widetilde{P}_{si}$, self-interference always decreases by an amount greater than or equal to the amount of decrease in downlink receive power. The following theorem characterizes the regime where the amount of self-interference reduction equals the amount of reduction in downlink receive power.

Theorem 1: Let $\mathbf{R}_{max}$ be a right inverse such that,

$$\mathbf{R}_{max} = \begin{cases} \mathbf{H}_d^{\dagger} - \mathbf{H}_n \mathbf{X}_m & \text{when } K > M_t - M_r \\ \mathbf{H}_d^{\dagger} - \mathbf{H}_n \mathbf{X}'_m & \text{when } K \leq M_t - M_r \end{cases} \tag{18}$$

where, $\mathbf{X}_m = \left(\left(\overline{\mathbf{H}}_s \mathbf{H}_n \right)^H \overline{\mathbf{H}}_s \mathbf{H}_n \right)^{-1} \left(\overline{\mathbf{H}}_s \mathbf{H}_n \right)^H \overline{\mathbf{H}}_s \mathbf{H}_d^{\dagger}$ and $\mathbf{X}'_m$ is the solution of the following program

$$\begin{aligned} &\min_{\mathbf{X}} \ \|\mathbf{H}_d^{\dagger} - \mathbf{H}_n \mathbf{X}\|_F \\ &\text{such that } \overline{\mathbf{H}}_s (\mathbf{H}_d^{\dagger} - \mathbf{H}_n \mathbf{X}) = \mathbf{0} \end{aligned} \tag{19}$$

For the self-interference suppressing precoder given in (15), if the desired per-user downlink receive power p_{dl} is such that,

$$p_{dl} \leq \frac{1}{\|\mathbf{R}_{max}\|_F^2} \tag{20}$$

then, $\sqrt{p_{dl}} \mathbf{R}_{max}$ is a solution of (15).

Proof. See Appendix (A). □

Let

$$p_{max} = 1/\|\mathbf{R}_{max}\|_F^2 \text{ and } \mathbf{P}_{max} = \frac{\mathbf{R}_{max}}{\|\mathbf{R}_{max}\|_F} = \sqrt{p_{max}} \mathbf{R}_{max}, \tag{21}$$

The theorem implies that when the desired per-user downlink receive power is lower than p_{max}, the optimal precoding strategy is to use $\mathbf{P}_{max}$ as the precoder and then adjust the total transmit power to p_{dl}/p_{max}. For example, if the desired per-user downlink receive power is 10 dB lower than p_{max}, then $\mathbf{P}_{max}/\sqrt{10}$ is the optimal precoder (recall that in our system the Frobenius norm of precoder is the total transmit power of base-station).

2) Precoder design algorithm: Algorithm 2 designs the precoder that near-optimally trades off self-interference and downlink receive power. First, multiple self-interference suppressing precoders are designed, where each precoder results in distinct self-interference and downlink receive power levels. Then, the precoder which best meets the desired levels is chosen. The number of self-interference suppressing precoders that Algorithm 2 need to design is reduced to a very few, based on the following two observations.

1) The precoder $\mathbf{P}_{max}$ in (21) can be used to generate the tradeoff for all downlink receive power levels lower than that of $\mathbf{P}_{max}$, using Theorem 1. In Algorithm 2, this observation is utilized in Step 3.

2) For all the downlink receive power levels greater than that of $\mathbf{P}_{max}$, downlink receive power can be increased in discrete steps, starting from that of $\mathbf{P}_{max}$ till $p_{dl}^{\dagger}$. Then, self-interference suppressing precoder in (15) can be used to get an optimal precoder for each downlink receive power level. Since self-interference monotonically increases with p_{dl} for self-interference suppressing precoders, the optimal self-interference power is less than the difference between the self-interference of two successive steps. Step 4 is based on this observation, in Algorithm 2.

Algorithm 2 Precoder design algorithm

Output precoder: $\mathbf{P}^*$

1: Compute the self-interference and per-user downlink receive powers required to achieve the demand rates using SINR expressions in (6). Let them be P_{si}^{dem} and p_{dl}^{dem}, respectively.
2: Let $\mathbf{P}_1$ be the self-interference suppressing precoder obtained by using $p_{dl} = p_{dl}^{dem}$ in (15). If the achieved uplink rate is greater than or equal to α_u^{dem}, then $\mathbf{P}^* = \mathbf{P}_1$. Continue to step 3, if the achieved uplink rate is less than α_u^{dem} or if the precoder generator program is infeasible for p_{dl}^{dem}.
3: Compute P_{si}^{max} and p_{dl}^{max} which are, respectively, the self-interference and downlink receive power for the precoder $\mathbf{P}_{max}$ given in (21).
4: On the line segment between the points $(0, 0)$ and $(p_{dl}^{max}, P_{si}^{max})$, find the point which is closest to the tuple $(p_{dl}^{dem}, P_{si}^{dem})$. Let the closest point be $(\widehat{p}_{dl}, \widehat{P}_{si})$. The corresponding precoder is, $\mathbf{P}_2 = \dfrac{\widehat{p}_{dl}}{p_{dl}^{max}}\mathbf{P}_{max}$.
5: Increase the per-user downlink receive power, in steps of Δ dB, from p_{dl}^{max} to $p_{dl}^{\dagger}$. Obtain the self-interference suppressing precoders for each of the per-user downlink receive power levels and compute compute their respective achievable rates. Let $\widetilde{p}_{dl}$ gives the rates closest to demand rates and let the corresponding precoder be $\mathbf{P}_3$.
6: If the rates of $\mathbf{P}_2$ are closer to the demand rates than that of $\mathbf{P}_3$, then $\mathbf{P}^* = \mathbf{P}_2$. Else, $\mathbf{P}^* = \mathbf{P}_3$.

If the outcome of the configuration design algorithm, $(\mathcal{S}_{HDT}^*, \mathcal{S}_{FD}^*)$, is an optimal configuration i.e., if $(\mathcal{S}_{HDT}^*, \mathcal{S}_{FD}^*)$ is a solution of the problem stated in (5), then we can claim the following about the optimality of the precoder design algorithm

- If $\mathbf{P}^* = \mathbf{P}_1$, the resulting rates are optimal. This is because the precoder design algorithm stops after Step 2 only when the achievable rates are greater the demand rates.

- If $\mathbf{P}^* = \mathbf{P}_2$, then the resulting rates are optimal. This is due to theorem 1.
- If $\mathbf{P}^* = \mathbf{P}_3$, the resulting downlink receive power is within a radius of $\Delta/2$ about its optimal value.

IV. Experimental evaluation

In this section, we discuss a systematic evaluation of JointNull using measured channel data from [13]. We first evaluate the precoder and configuration design algorithms for the case of $N_{ac} = 0$, allowing direct comparisons with SoftNull [13]. Then, we evaluate the case $N_{ac} \geq 0$. Specifically, we study the two parameters related to analog cancelers that impact the performance of JointNull: the *quality* of analog cancelers and the *number* of analog cancelers. We use β_{ac} dB to measure the quality of an analog canceler, where higher β_{ac} means higher suppression and hence better quality. We conclude the section by giving the rate region of JointNull and comparing it with half-duplex TDD.

For the case of $N_{ac} = 0$, we will compare with SoftNull [13] that computes precoder for a given configuration (consisting of transmit-only and receive-only antennas since $N_{ac} = 0$) and a parameter which represents number of degrees of freedom available for the precoder; hence SoftNull decouples the self-interference suppression from downlink beamforming. In [13], to analyze SoftNull, a configuration is chosen for each M_t such that the transmit antennas are selected column-wise from the left side of the array. For example, when $M_t = 24$, the three leftmost columns of antennas of the 8×9 antenna array are chosen as transmit antennas.

We use the channel measurements from Argos [14] massive MIMO array collected by the authors of [13]. More details on the experimental setup are provided in [13], where the Argos array had 72 antennas in an 8×9 antenna array configuration with four uplink and four downlink users i.e., $M = 72$, $M_{row} = 8$, $M_{col} = 9$ and $K = 4$. The number of partitions for the array, $|\mathcal{B}_{JN}| = 422$. To simulate downlink and uplink rates, we assume that the total base station power is 0 dBm and the user transmit power is -10 dBm in outdoor channel conditions and -20 dBm in indoor channel conditions. The noise floor is assumed to be at -95 dBm, at both the base station and the users.

The amount of self-interference that can be canceled after digitizing the received signal depends on the impairments in the transceiver chain, such as transmit noise, IQ-imbalance, ADC quantization noise, thermal noise and the distortions due to non-linearities of power amplifier and other analog circuits [16]–[19]. We assume that the total residual self-interference power

after digital cancelation is 25 dB below the self-interference levels achieved from JointNull i.e., $\beta_{dc} = 25$ dB. Transmitter with better circuitry and more accurate clocks would allow the digital cancelers to cancel a larger amount of self-interference, resulting in higher achievable rates [19].

A. Array with no analog cancelers, $N_{ac} = 0$

We first evaluate the JointNull precoder, by considering the case with a fixed configuration. Then, we evaluate the combined gains of antenna configuration and precoder design algorithms.

1) Fixed configuration: JointNull trades off self-interference and downlink receive power when the configuration is fixed. Figure 3a gives the tradeoff between between self-interference and downlink receive power for the self-interference suppressing precoder in (15) and SoftNull, in indoor and outdoor channels conditions. The configuration for Figure 3a has $M_t = 36$ transmit antennas, the tradeoffs for self-interference suppressing precoder for configurations with $M_t = \{10, 20, 30\}$ are given in Figure 3b.

The self-interference suppressing precoder in (15) is optimal for a fixed downlink receive power. However, SoftNull precoder is sub-optimal for the following reason. Let $\mathbf{H}_s = \mathbf{USV}^H$ be the SVD decomposition of $\mathbf{H}_s$, where $\mathbf{S} \in \mathbb{C}^{M_r \times M_t}$, $\mathbf{V} \in \mathbb{C}^{M_t \times M_t}$ and $\mathbf{U} \in \mathbb{C}^{M_r \times M_r}$. SoftNull precoder restricts the downlink transmissions to a few low-power eigen directions of $\mathbf{H}_s$, thus reducing self-interference. For example, if the columns of $\mathbf{P}$ lie in the subspace spanned by the last n columns of $\mathbf{V}$, then the self-interference cannot exceed that of sum of squares of the least n singular values in $\mathbf{S}$. However, the high-power eigen directions remain unused for downlink transmissions, even if they are orthogonal to the downlink channel, $\mathbf{H}_d$.

In indoor channel conditions, the users are close to the base-station and consequently, pathloss is low. Thus, downlink receive power, for a given self-interference power, is higher than that for outdoor conditions. However, the outdoor curve is steeper than indoor curve, for $p_{dl} \geq p_{max}$. As steepness increases, more self-interference gets suppressed for a fixed amount of downlink receive power loss. For example, as shown in Figure 3a, when the achieved self-interference level is 40 dB below transmit power, 3 dB loss in downlink receive power results in 18 dB and 12 dB of additional self-interference suppression for the outdoor and indoor channels, respectively. Equivalently, reducing the downlink rate by 1 bps/Hz increases the uplink rate by about 6 bps/Hz and 4 bps/Hz in outdoor and indoor channel conditions, respectively, when the achieved self-interference levels are 40 dB below the transmit power. As noted in [13], indoor channels have

more backscattering than the outdoor channels and hence, the tradeoff curve for indoor channels is less steep than the outdoor curve.

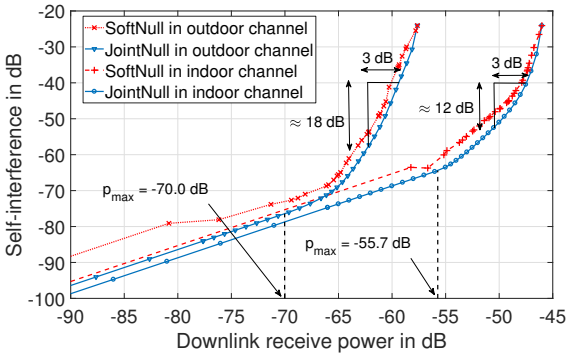

(a) *JointNull and SoftNull comparison for a configuration with $M_t = M_r = 36$. The self-interference reduction and downlink receive power reduction are equal for JointNull when $p_{dl} \leq p_{max}$ i.e., tradeoff curves are linear with unit slope for $p_{dl} \leq p_{max}$.*

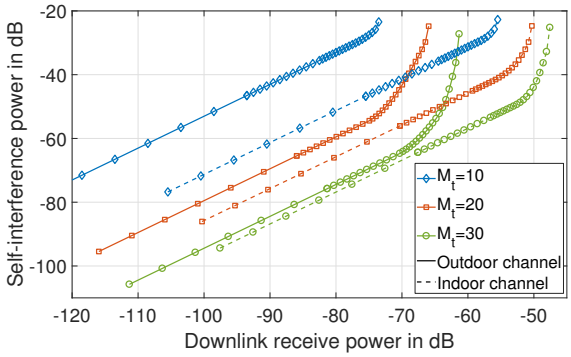

(b) *Self-interference suppression and downlink receive power of JointNull for the configurations with $M_t = \{10, 20, 30\}$ in outdoor channel conditions.*

Large self-interference reductions are at the right half of the Figure 3a and 3b, where the curves are steeper. From Theorem 1, when $p_{dl} \leq p_{max}$, the tradeoff curves have unit slope i.e., amount of self-interference suppression is equal to the amount of downlink receive power reduction. For example, in Figure 3a, p_{max} for indoor and outdoor channels are about -55.7 dB and -70.02 dB, respectively and the self-interference suppression gains are trivial for $p_{dl} \leq p_{max}$. Hence, the following inference.

Inference 1a: The tradeoff between self-interference and downlink receive power is more favorable when downlink receive power is larger than p_{max}, given by (21).

2) Combined gains of configuration and precoder design algorithms: In Figure 4, the downlink power is fixed for SoftNull, for all the configurations. The x-axis of the Figure 4 is the number of transmit antennas in the configuration used by SoftNull. JointNull designs a precoder and configuration that minimizes the self-interference, while achieving the same levels of downlink and uplink receive powers as that of the corresponding SoftNull precoder. JointNull outperforms SoftNull due to two reasons. First, for any fixed antenna configuration, JointNull precoder is optimal. Second, JointNull chooses a configuration based on channel conditions, the desired downlink and uplink receive power, unlike SoftNull which has one fixed configuration

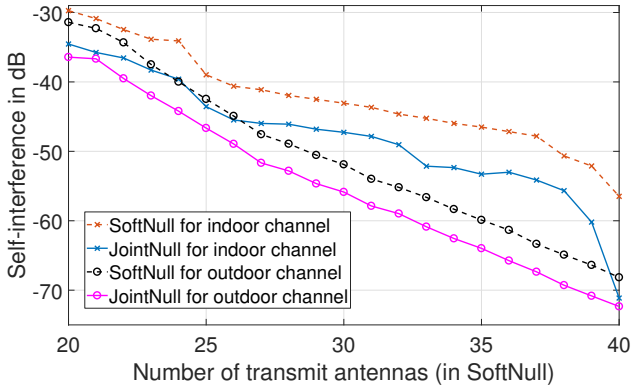

Fig. 4: *Downlink receive power is fixed. The x coordinate is the number of transmit antennas for the SoftNull. The curves labeled 'JointNull' give the self-interference achieved by JointNull with the downlink and uplink receive power same as that of the corresponding SoftNull precoder.*

for each M_t. JointNull can suppress up to 15 dB of additional self-interference compared to SoftNull.

B. Array with $N_{ac} \geq 0$

Figure 5 gives the self-interference of JointNull when $N_{ac} > 0$, for the same simulation settings as that for the Figure 4. The addition of analog cancelers further improves the self-interference suppression levels of JointNull, in contrast to the case with $N_{ac} = 0$ in Figure 4. For a fixed uplink receive power, the number of transmit antennas (M_t) increases with N_{ac}. The maximum achievable downlink receive power increases with M_t. Thus, for a fixed downlink receive power, the amount of downlink receive power that can be sacrificed for suppressing self-interference increases with M_t. Hence, in Figure 5 self-interference decreases with increasing N_{ac}.Note that there is a cross-over point for indoor and outdoor for both $N_{ac} = 5, 10$. After the cross-over point, the indoor self-interference reduces much faster than the outdoor channels. The main reason for this behavior is that the maximum achievable downlink receive power increases faster in indoor conditions than in outdoor conditions, with the increase in transmit antennas (due to low pathloss in indoor conditions). At the crossover point, the self-interference is same for both the indoor and outdoor conditions. Beyond the crossover point, the amount of downlink receive power which can be sacrificed towards self-interference suppression is higher in indoor conditions than in outdoor conditions, and hence, the self-interference in indoor conditions decreases faster than in outdoor conditions.

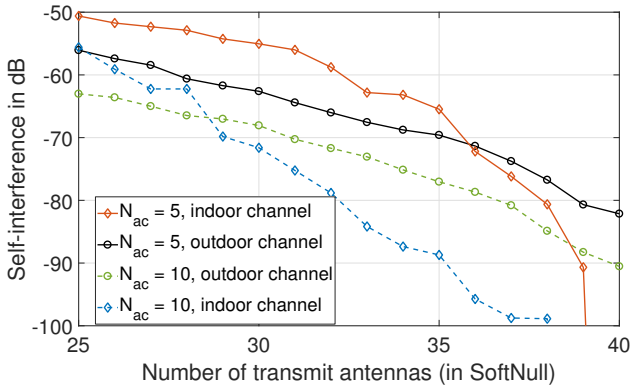

Fig. 5: *For the analog cancelers, $\beta_{ac} = 40$ dB. Self-interference for indoor channel decreases faster than outdoor channel after cross-over point.*

In Figure 6, we study how varying the number or quality of analog cancelers influences the JointNull. The self-interference power/reduction plots, Figures 3a-5, give insights on workings of the precoder and configuration design algorithms, but they do not convey the gains against half-duplex. For example, as the number of half-duplex transmit antennas increases, the amount of self-interference suppression increases, but the uplink receive power also decreases due to reduced receiver processing gain. Thus, uplink rates may not increase by better self-interference suppression alone. The advantages of JointNull, relative to half-duplex, is captured by comparing the achievable rate, which is a function of self-interference, downlink and uplink receive power. The maximum achievable sum-rates of JointNull for $N_{ac} = 0, 1, \cdots, 72$ with $\beta_{ac} = 20$, 40 and 60 dB, in both outdoor and indoor channel conditions are given in Figure 6.

With more analog cancelers, N_{ac}, the number of receive antennas increases and hence the dimension of the self-interference sub-space also increases. But since the number of transmit antennas is also increasing with N_{ac}, the dimension of transmit space too increases. Additionally, the quality of analog cancelers impacts the power in the self-interference subspace. Figures 6 shows the impact of quality and number of analog cancelers on the sum-rate. When analog cancelers are of high quality, e.g. $\beta_{ac} = 60$dB, the self-interference on full-duplex antennas is quite low and hence the transmit antennas have to largely suppress self-interference on half-duplex receive antennas, leading to performance which increases monotonically with N_{ac}. But, when analog cancelers are of low quality, the burden of suppressing a large amount of self-interference on full-duplex antennas falls upon transmit precoding, leading to a maximal rate

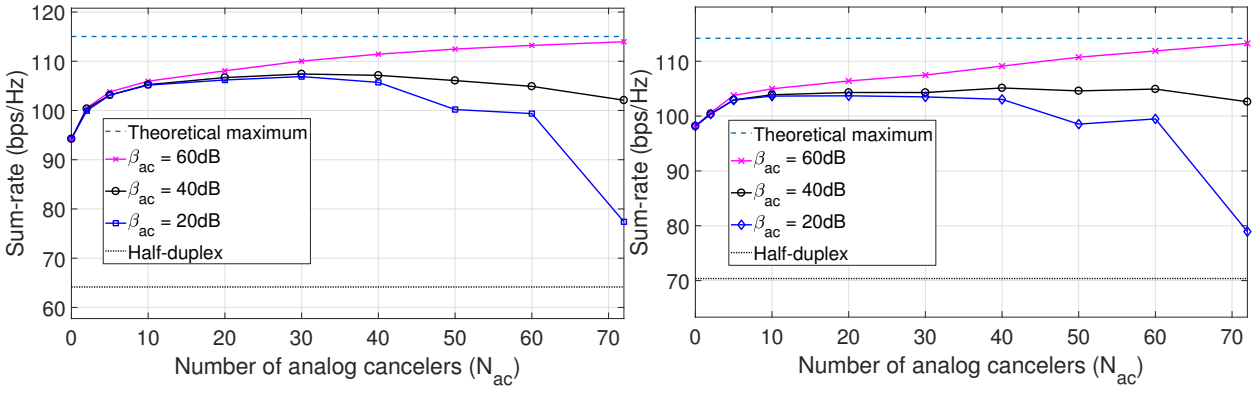

(a) Outdoor channel conditions

(b) Indoor channel conditions

Fig. 6: *The N_{ac} that achieves maximal sum-rate with JointNull depends on both the quality of analog cancelers and the channel conditions.*

point where $N_{ac} < M$. That is, JointNull is better off without a large number of low quality analog cancelers. When transmit antennas beam a null at a half-duplex receive antenna, the precoder manipulates the phase and amplitude of the signals of transmit antennas such that the signals add destructively at the receive antenna. The destructive addition or self-interference suppression by beamforming requires at least two transmit antennas, and the suppression happens at the air-antenna interface of the receive antenna. However, the self-interference at a full-duplex antenna due to its own transmissions cannot be suppressed by beamforming. This is because the self-interference from its very own transmissions at a full-duplex antenna is the leaked transmit signal in the receive path of the antenna, as circulator provides poor isolation between in-band transmit and receive paths. The self-interference signal never leaves the full-duplex antenna. Hence, irrespective of the phase and amplitude changes, the same proportion of the transmit signal leaks into the receive path and thus, "irreducible" for the self-interference suppressing precoder Adding a large number of low quality analog cancelers, greatly increases the amount of irreducible self-interference. Inference 2a is drawn from this argument and the results in Figure 6.

Inference 2a: There exists an optimal number of analog cancelers, which could be less than the total number of antennas. Using more than the optimal number of analog cancelers decreases the achievable sum-rates. For high quality analog cancelers, the optimal number of analog cancelers is close to the number of antennas, and for low quality analog cancelers, the optimal number is

much lower than the number of antennas.

The rate gains diminish with the increasing number of analog cancelers, as depicted in Figure 6. For the case with $\beta_{ac} = 20$ dB, at $N_{ac} \approx 30$ the sum-rate reaches the maximum, which is 107 bps/Hz and 104 bps/Hz in outdoor and indoor conditions, respectively; note that this maximum is *not* the rate of ideal full-duplex. Interestingly, more than 99% of the maximum (107 or 104 bps/Hz) is achieved with only ten analog cancelers, for both outdoor as well as indoor conditions. For the case with $\beta_{ac} = 60$ dB, when $N_{ac} \geq 40$, the sum-rate is greater than or close to 99% of the maximum rate possible with 60 dB cancelers. It should be noted that the maximum for $\beta_{ac} = 20$ dB is more than 90% of the ideal full-duplex rate and the maximum rate for $\beta_{ac} = 60$ dB is more than 99% of the ideal full-duplex rate. Near-optimal sum rates can be achieved using a fewer number of analog cancelers than the respective optimal number. Hence, the following inference.

Inference 2b: For a given quality of analog canceler, near-maximal performance can be achieved with the number of analog cancelers that is much lesser than the corresponding optimal number; here the maximum is dependent on the quality of analog cancelers.

C. Achievable rate regions with JointNull

The achievable rate regions of JointNull are given in Figure 7 for the cases $N_{ac} = 40,\ 30,\ 10$ and 0. The quality, $\beta_{ac} = 60,\ 40$ and 20 dB. respectively, for the cases with $N_{ac} = 40,\ 30$ and $N_{ac} = 10$. The quality and the number of analog cancelers are chosen such that the achievable sum-rates are greater than or close to 99% of their respective maximum sum rates (see Figure 6). The rate region for TDD is also given in the Figure 7, to elucidate the rate gains of JointNull against half-duplex. Figure 7a and 7b give the rates in indoor and outdoor channel conditions, respectively. The achievable rate region of JointNull is generated by first computing the rates for all self-interference suppressing precoders obtained with $p_{dl} \in \{0, p_{dl}^{\dagger}/n, 2p_{dl}^{\dagger}/n, \cdots, p_{dl}^{\dagger}\}$ (for a large n), for each configuration of $\mathcal{B}_{JN}$ and then interpolating the boundary. The rate region of JointNull is same as the rate region of an optimal full-duplex scheme, which is allowed to use only the configurations in $\mathcal{B}_{JN}$ i.e., the rate region for the problem (5) with $\mathbb{B} = \mathcal{B}_{JN}$.

The configurations with $M_t >> M_r + K$, achieve their best possible uplink-rates, by only a small reduction in downlink-rates. The reason is as follows. Let $\mathbf{H}_s = \mathbf{USV}^H$ be the SVD of $\mathbf{H}_s$. The last $M_t - M_r$ columns of $\mathbf{V}$ are right-orthogonal to $\mathbf{H}_s$. Hence, when $M_t > M_r + K$

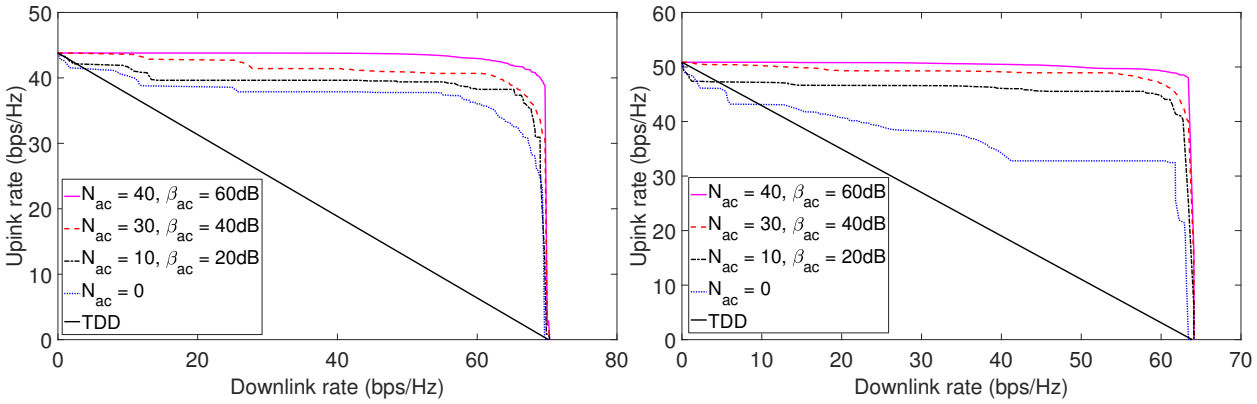

(a) Indoor channel conditions

(b) Outdoor channel conditions

Fig. 7: *Comparing JointNull achievable rates with TDD*

there are at least K directions which are orthogonal to $\mathbf{H}_s$. Any downlink transmissions in these K directions ensure zero self-interference. If $M_t = M_r + K$, then there are exactly K directions or K downlink degrees of freedom for achieving zero self-interference. When $M_t >> M_r + K$, the number of such downlink degrees of freedom is much higher than the number of downlink users i.e., $M_t - M_r >> K$. When downlink demand is much higher than uplink demand, which would require $M_t >> M_r$, the precoder alone can suppress a large amount of self-interference by sacrificing only a little of downlink receive power. In such a case, where downlink demand is much higher than uplink demand, even the good quality analog cancelers result in marginal gains. Hence, in Figure 7, the achievable downlink rate for JointNull with $N_{ac} = 0$ is within 99% of the maximum downlink rate when the desired uplink rate is less than 50% of the maximum uplink rate. When the demand is nearly symmetrical or biased towards uplink, adding analog cancelers helps, as can be observed in the Figure 7b. This is because, in such cases either $M_t \sim M_r$ or $M_t < M_r$. This argument entails Inference 2a.

Inference 3: JointNull requires a very few or no analog cancelers when the demand is highly biased towards downlink.

V. Conclusion

In this paper, we discussed a new flexible architecture which uses a few reconfigurable analog cancelers to convert some antennas of a large array into full-duplex antennas. Combined with transmit precoding, the proposed scheme JointNull achieves significant rate gains compared

to half-duplex or previously proposed schemes. Thus, the new architecture provides a flexible tradeoff between analog complexity and overall performance gains.

APPENDIX A
PROOF OF THEOREM (1)

We rewrite the objective of (15) as

$$f(\mathbf{X}) = \|\mathbf{Y} - \mathbf{A}\mathbf{X}\|_F, \tag{22}$$

where $\mathbf{Y} = \overline{\mathbf{H}}_s\mathbf{H}_d^{\dagger}$ and $\mathbf{A} = \overline{\mathbf{H}}_s\mathbf{H}_n\mathbf{X}$. When $K > M_t - M_r$, unconstrained minimization of $f(\mathbf{X})$ is a least-squares problem and $\mathbf{X}_m = (\mathbf{A}^H\mathbf{A})^{-1}\mathbf{A}^H\mathbf{Y}$, is the solution. Let the corresponding right inverse be $\mathbf{R}_{max} = \mathbf{H}_d^{\dagger} - \mathbf{H}_n\mathbf{X}_m$. Since $\mathbf{X}_m$ minimizes $\|\mathbf{Y} - \mathbf{A}\mathbf{X}\|_F^2$,

$$\|\mathbf{Y} - \mathbf{A}\mathbf{X}_m\|_F < \|\mathbf{Y} - \mathbf{A}\mathbf{X}\|_F, \ \forall \ \mathbf{X} \neq \mathbf{X}_m \tag{23}$$

$$\implies \|\mathbf{H}_s\mathbf{R}_{max}\|_F < \|\mathbf{H}_s\mathbf{R}\|_F \ \forall \ \mathbf{R} \neq \mathbf{R}_{max}, \text{ if } K > M_t - M_r. \tag{24}$$

Let $\mathbf{H}_s = \mathbf{U}\mathbf{S}\mathbf{V}^H$ be the SVD of self-interference channel matrix. When $K \leq M_t - M_r$, any right inverse of $\mathbf{H}_d$ whose columns lie in the subspace spanned by the last $M_t - M_r$ columns of $\mathbf{V}$ is orthogonal to $\mathbf{H}_s$ and hence, the resulting self-interference is zero. The solution of (19) gives the right inverse which has the least Frobenius norm among all the right inverses which are orthogonal to $\mathbf{H}_s$. Let $\mathbf{R}_{max} = \mathbf{H}_d^{\dagger} - \mathbf{H}_n\mathbf{X}'_m$, when $K \leq M_t - M_r$.

$$\|\mathbf{H}_s\mathbf{R}_{max}\|_F = 0 \leq \|\mathbf{H}_s\mathbf{R}\|_F, \ \forall \ \mathbf{R} \neq \mathbf{R}_{max}, \text{ if } K \leq M_t - M_r \tag{25}$$

If $p_{dl} \leq 1/\|\mathbf{R}_{max}\|_F^2$, then

$$\|\sqrt{p_{dl}}\mathbf{R}_{max}\|_F \leq \left\| \frac{1}{\|\mathbf{R}_{max}\|_F}\mathbf{R}_{max} \right\|_F = 1 \tag{26}$$

Hence, $\sqrt{p_{dl}}\mathbf{R}_{max}$ satisfies the constraint of (15).

From (24) and (25),

$$\|\mathbf{H}_s\mathbf{R}_{max}\|_F \leq \|\mathbf{H}_s\mathbf{R}\|_F \ \forall \ \mathbf{R} \neq \mathbf{R}_{max} \tag{27}$$

$$\implies \|\mathbf{H}_s(\sqrt{p_{dl}}\mathbf{R}_{max})\|_F \leq \|\mathbf{H}_s(\sqrt{p_{dl}}\mathbf{R})\|_F \ \forall \ \mathbf{R} \neq \mathbf{R}_{max} \tag{28}$$

Hence, $\sqrt{p_{dl}}\mathbf{R}_{max}$ is a solution of (15).

APPENDIX B
ALGORITHM FOR CONSTRUCTING SET, $\mathcal{B}_{JN}$, OF ANTENNA CONFIGURATIONS WITH LOW SELF-INTERFERENCE

The full-duplex antennas experience less self-interference than half-duplex receive antennas. So, we first assume that there are zero full-duplex antennas and choose the partitions which could result in low self-interference on half-duplex receive antennas. Then, N_{ac} of half-duplex transmit antennas are chosen as full-duplex antennas.

We first note that the self-interference on a receive antenna increases with the decrease in its distance from the transmit antennas, due to pathloss. Also, the experimental studies in [13] have shown that a larger amount of self-interference can be suppressed using precoders when the arrays have contiguous half-duplex transmit and receive antenna partitions. By following the rules of thumb given below, sequentially, we choose partitions for each $M_t \in \{1, \cdots, M-1\}$.

1) Transmit and receive antennas are contiguous.
2) The number of pairs of neighboring transmit and receive antennas is the least.
3) The number of receive antennas which neighbor the transmit antennas is the least.

We represent the antenna partitions as depicted in Figure 8 and assume that each block in the grid is a square whose side length is unity. We represent half-duplex transmit antennas by white blocks and half-duplex receive antennas by gray blocks. Figure 8 depicts a 4×5 antenna arrays. The set, $\mathcal{S}_{HDT}$, indexes the white blocks, which are the transmit antennas. For example, for the array in Figure 8d, $\mathcal{S}_{HDT} = \{(1,1),(1,2),(2,1),(2,2),(3,1),(4,1)\}$. The number of pairs of neighbors is the number of edges that are shared by both the gray and white blocks. For example, arrays in Figure 8a and 8b have eight and four shared edges, respectively. The number of neighboring gray blocks is the number of gray blocks which share at least one edge with white blocks. For example, there are four shared edges in both Figure 8e and 8f, but they have four and three neighboring gray blocks, respectively.

Let the set $\mathcal{B} \subset \mathbb{B}$ contain all the half-duplex partitions that satisfy the aforementioned rules of thumb, for all M_t. The algorithm to construct $\mathcal{B}$ is given in Algorithm 3. The algorithm is based on the following observations.

1) The number of edges shared between white and gray blocks cannot be less than that of the least-perimeter rectangle which contains all the white blocks. A rectangle which contains all the white blocks has the least-perimeter if it has at least one white block in every row

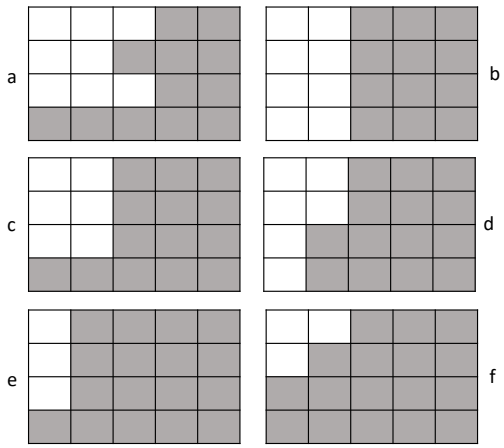

Fig. 8: *Partitions for* $M_t = 8, 6$ *and* 3.

and column. For example, in Figure 8a, the least-perimeter rectangle is the $3\times$ 3 rectangle at the top left corner.

2) For a rectangle that contains one corner block, the number of shared edges are half the rectangle's perimeter (for example, Figure 8c, e and f). The number of shared edges for a rectangle which contains two corner blocks is equal to the length between the corners (for example, Figure 8b).
3) The number of shared edges, when white blocks are in contiguous columns (for example, Figure 8d and b) is M_{row} if the number of white blocks is divisible by M_{row}. It is $M_{row}+1$, if the number of white blocks is not divisible by M_{row}.
4) Any block can be arranged such that it has no more than two shared edges. For example, in Figure 8a, a white block, and a gray block have three shared edges. By moving the rightmost white block in the third row to the second row, every block will have utmost two shared edges.
5) For a fixed number of white blocks, among the partitions which have the same number of shared edges, the partitions which have the largest number of gray blocks with two shared edges have the largest number of gray blocks without any shared edge (for example, compare Figure 8e and f).

A partition cannot have the least number of shared edges if no corner block is a white one or the partition has at least one block with more than two shared edges. Since the length of each block is unity, the length and the area of any rectangle in the array would be a positive integer.

Algorithm 3 Algorithm to construct $\mathcal{B}$

Output: $\mathcal{B}$ [h]

for $j = 1, \;\; j \leq M/2, \;\; j{+}{+}$ **do**

  $\mathcal{F}_j = \{(M_{row}, \lceil j/M_{row} \rceil)\}$

  if $0 \equiv j \mod M_{row}$ **then** $N_{neigh}(j) = M_{rows}$; **else** $N_{neigh}(j) = M_{row} + 1$ **end if**

  $\mathcal{F}'_j = \{(a_i, b_i) : a_i \times b_i = j \text{ and } 0 < a_i, b_i < M_{row}\}$

  $\mathcal{Q}_j = \{a_i + b_i : (a_i, b_i) \in \mathcal{F}'_j\}$.

  if $\min(\mathcal{Q}_j) = N_{neigh}(j)$ **then**

    $\mathcal{F}_j = \mathcal{F}_j \cup \{(a_i, b_i) : a_i + b_i = N_{neigh}(j) \text{ and } (a_i, b_i) \in \mathcal{F}'_j\}$

  end if

  if $\min(\mathcal{Q}_j) < N_{neigh}(j)$ **then**

    $N_{neigh}(j) = \min(\mathcal{Q}_j)$

    $\mathcal{F}_j = \{(a_i, b_i) : a_i + b_i = N_{neigh}(j) \text{ and } (a_i, b_i) \in \mathcal{F}'_j\}$

  end if

end for

for $M_t = 1, \;\; M_t \leq M/2, \;\; M_t{+}{+}$ **do**

  Find the rectangles which can contain M_t gray blocks and have the least number of shared edges,

$$\mathcal{I}_{M_t} = \left\{ n : N_{neigh}(n) \leq N_{neigh}(i) \;\forall\; M_t \leq n, i \leq \left\lceil \sqrt{M_t} \right\rceil^2 \right\}.$$

  For all $n \in \mathcal{I}_{M_t}$, construct $\mathcal{S}^k_{HDT} = \{(r_i, c_i) : r_i \leq a_j, c_i \leq b_j \, (a_j, b_j) \in \mathcal{F}_n\}$, such that $|\mathcal{S}^k_{HDT}| = M_t$, no block in $\mathcal{S}^k_{HDT}$ shares three or more of its edges with differently colored blocks and each $\mathcal{S}^k_{HDT}$ has at least one white corner block. Let the number of such sets be L_s and $\mathcal{D} = \{\mathcal{S}^k_{HDT} : k = 1, \cdots, L_s\}$.

  Let $\mathcal{S}^K_{HDT} \in \mathcal{D}_{HDT}$ has the largest number of gray blocks with two shared edges. Construct $\mathcal{D}_{HDT} \subset \mathcal{D}$, such that the number of gray blocks with two shared edges in every $\mathcal{S}^k_{HDT} \in \mathcal{D}_{HDT}$ is same as that of $\mathcal{S}^K_{HDT}$.

  $\mathcal{B}^n_{M_t} \leftarrow \mathcal{D}_{HDT}, \;\forall n \in \mathcal{I}_{M_t}$

  $\mathcal{B}^n_{M-M_t} \leftarrow \mathcal{D}'_{HDT}$, where $\mathcal{D}'_{HDT}$ is obtained by using transmit antennas as receive antennas and vice-versa in $\mathcal{D}_{HDT}$.

end for

$\mathcal{B} \leftarrow \{(\mathcal{B}^n_{M_t}, \Phi) : M_t = 1, \cdots, M \text{ and } n \in \mathcal{I}_{M_t}\}$. Since there are no full-duplex antennas, null set is the second element in each of the tuple.

A rectangle with length a and width b can be uniquely mapped to a tuple (a, b), when a and b are both integers. The number of shared edges are $a + b$, and the maximum number of white blocks the rectangle can accommodate is ab.

Let the number of white blocks be j. The problem of finding the least-perimeter rectangle which can accommodate j white blocks is equivalent to finding the integer tuple(s) (a^*, b^*) such that, $a^*b^* \geq j$ and $a^* + b^* \leq a_i + b_i$, for all $a_i b_i \geq j$, where, $a^*, a_i \leq M_{row}$ and $b^*, b_i \leq M_{col}$. There can be multiple such tuples for a given j. For example when $j = 7$, the tuples are $(2, 4)$, $(4, 2)$ and $(3, 3)$. The 3^{rd} observation puts an upper bound on the sum i.e., $a^* + b^* \leq M_{row} + 1$. If there exists no tuple, (a, b), such that $a + b \leq M_{row} + 1$, then $(a^*, b^*) = (M_{row}, \lceil j/M_{row} \rceil)$.

In the algorithm, the tuples with the least sum, for each $j = 1, \cdots, M/2$, are computed from step 1 through step 13. After Step 13, the algorithm finds the rectangles with the least number of shared edges for each $M_t = 1, \cdots, M - 1$. By tightly packing the white blocks in each of the rectangles, a partition is generated with the least number of shared edges and all such partitions are added to the set $\mathcal{B}$.

We have assumed that the number of antennas is even and $M_{row} \leq M_{col}$. The algorithm requires a few minor changes, for the case with an odd number of antennas. For a given antenna array, the set $\mathcal{B}$ does not change. Hence, $\mathcal{B}$ can be computed once and stored in a look-up table.

The half-duplex transmit antennas are converted into full-duplex antennas, based on the following two observations,

1) Better receive diversity is achieved when the receive antennas are widely separated.
2) As analog-cancelers cancel much of the self-interference on full-duplex antennas, an optimal precoder would suppress much less self-interference on full-duplex antennas than on half-duplex receive antennas.

The half-duplex transmit antennas that are farthest from the half-duplex receive antennas are chosen as full-duplex antennas as they result in better receive diversity. Let $\mathcal{A}^n_{M_t} \subset \mathcal{B}^n_{M_t}$ be a set such that $|\mathcal{A}^n_{M_t}| = N_{ac}$ and no antenna in $\mathcal{B}^n_{M_t} \setminus \mathcal{A}^n_{M_t}$ is closer than any antenna in $\mathcal{A}^n_{M_t}$, where $\mathcal{B}^n_{M_t}$ is given in Algorithm 3. The set, $\mathcal{B}_{JN}$, is obtained by replacing the null set with $\mathcal{A}^n_{M_t}$ in Step 21 of Algorithm 3.

REFERENCES

[1] N. M. Gowda and A. Sabharwal, "Spatial half-duplex: Precoder design and experimental evaluation," in *2016 50th Asilomar Conference on Signals, Systems and Computers*, pp. 1322–1326, Nov 2016.

[2] A. Sabharwal, P. Schniter, D. Guo, D. W. Bliss, S. Rangarajan, and R. Wichman, "In-Band Full-Duplex Wireless: Challenges and Opportunities," *IEEE Journal on Selected Areas in Communications*, vol. 32, pp. 1637–1652, Sept 2014.

[3] M. Duarte and A. Sabharwal, "Full-duplex wireless communications using off-the-shelf radios: Feasibility and first results," in *Signals, Systems and Computers (ASILOMAR), 2010 Conference Record of the Forty Fourth Asilomar Conference on*, pp. 1558–1562, Nov 2010.

[4] J. I. Choi, M. Jain, K. Srinivasan, P. Levis, and S. Katti, "Achieving Single Channel, Full Duplex Wireless Communication," in *Proceedings of the Sixteenth Annual International Conference on Mobile Computing and Networking*, MobiCom '10, (New York, NY, USA), pp. 1–12, ACM, 2010.

[5] G. P. Achaleshwar Sahai and A. Sabharwal, "Pushing the limits of Full-duplex: Design and Real-time Implementation," *CoRR*, vol. abs/1107.0607, 2011.

[6] M. Duarte, C. Dick, and A. Sabharwal, "Experiment-Driven Characterization of Full-Duplex Wireless Systems," *IEEE Transactions on Wireless Communications*, vol. 11, pp. 4296–4307, December 2012.

[7] E. Aryafar, M. A. Khojastepour, K. Sundaresan, S. Rangarajan, and M. Chiang, "MIDU: Enabling MIMO Full Duplex," in *Proceedings of the 18th Annual International Conference on Mobile Computing and Networking*, Mobicom '12, (New York, NY, USA), pp. 257–268, ACM, 2012.

[8] M. Duarte, A. Sabharwal, V. Aggarwal, R. Jana, K. K. Ramakrishnan, C. W. Rice, and N. K. Shankaranarayanan, "Design and Characterization of a Full-Duplex Multiantenna System for WiFi Networks," *IEEE Transactions on Vehicular Technology*, vol. 63, pp. 1160–1177, March 2014.

[9] D. Bharadia and S. Katti, "Full duplex MIMO radios," in *11th USENIX Symposium on Networked Systems Design and Implementation (NSDI 14)*, pp. 359–372, 2014.

[10] J. Zhou, T. H. Chuang, T. Dinc, and H. Krishnaswamy, "Integrated Wideband Self-Interference Cancellation in the RF Domain for FDD and Full-Duplex Wireless," *IEEE Journal of Solid-State Circuits*, vol. 50, pp. 3015–3031, Dec 2015.

[11] X. Yang and A. Babakhani, "A Full-Duplex Single-Chip Transceiver With Self-Interference Cancellation in 0.13 μ m SiGe BiCMOS for Electron Paramagnetic Resonance Spectroscopy," *IEEE Journal of Solid-State Circuits*, vol. 51, pp. 2408–2419, Oct 2016.

[12] 3GPP Technical Reports TR 38.913 V14.1.0, "Study on Scenarios and Requirements for Next Generation Access Technologies," 2017.

[13] E. Everett, C. Shepard, L. Zhong, and A. Sabharwal, "SoftNull: Many-Antenna Full-Duplex Wireless via Digital Beamforming," *IEEE Transactions on Wireless Communications*, vol. 15, pp. 8077–8092, December 2016.

[14] C. Shepard, H. Yu, and L. Zhong, "ArgosV2: A Flexible Many-antenna Research Platform," in *Proceedings of the 19th Annual International Conference on Mobile Computing & Networking*, MobiCom '13, (New York, NY, USA), pp. 163–166, ACM, 2013.

[15] A. Wiesel, Y. C. Eldar, and S. Shamai, "Zero-Forcing Precoding and Generalized Inverses," *IEEE Transactions on Signal Processing*, vol. 56, pp. 4409–4418, Sept 2008.

[16] A. Sahai, G. Patel, C. Dick, and A. Sabharwal, "Understanding the impact of phase noise on active cancellation in wireless full-duplex," in *Proceedings of Asilomar Conference on Signals, Systems and Computers*, 2012.

[17] A. Sahai, G. Patel, C. Dick, and A. Sabharwal, "On the Impact of Phase Noise on Active Cancelation in Wireless Full-Duplex," *IEEE Transactions on Vehicular Technology*, vol. 62, pp. 4494–4510, Nov 2013.

[18] B. P. Day, A. R. Margetts, D. W. Bliss, and P. Schniter, "Full-Duplex Bidirectional MIMO: Achievable Rates Under Limited Dynamic Range," *IEEE Transactions on Signal Processing*, vol. 60, pp. 3702–3713, July 2012.

[19] E. Ahmed, A. M. Eltawil, and A. Sabharwal, "Rate Gain Region and Design Tradeoffs for Full-Duplex Wireless Communications," *IEEE Transactions on Wireless Communications*, vol. 12, pp. 3556–3565, July 2013.